ACS NANO

www.acsnano.org

ARTICLE

In Situ-Forming, Bioorthogonally Cross-linked, Nanocluster-Reinforced Hydrogel for the Regeneration of Corneal Defects

Nae-Won Kang, Kyeongwoo Jang, Euisun Song, Uiyoung Han, Youngyoon Amy Seo, Fang Chen, Thitima Wungcharoen, Sarah C. Heilshorn, and David Myung*

Cite This: *ACS Nano* 2024, 18, 21925–21938

Read Online

ACCESS | Metrics & More | Article Recommendations | Supporting Information

ABSTRACT: **Corneal defects can lead to stromal scarring and vision loss, which is currently only treatable with a cadaveric corneal transplant. Although *in situ*-forming hydrogels have been shown to foster regeneration of the cornea in the setting of stromal defects, the cross-linking, biomechanical, and compositional parameters that optimize healing have not yet been established. This, Corneal defects are also almost universally inflamed, and their rapid closure without fibrosis are critical to preserving vision. Here, an *in situ* forming, bioorthogonally cross-linked, nanocluster (NC)-reinforced collagen and hyaluronic acid hydrogel (NCColHA hydrogel) with enhanced structural integrity and both pro-regenerative and anti-inflammatory effects was developed and tested within a corneal defect model *in vivo*. The NCs serve as bioorthogonal nanocross-linkers, providing higher cross-linking density than polymer-based alternatives. The NCs also serve as delivery vehicles for prednisolone (PRD) and the hepatocyte growth factor (HGF). NCColHA hydrogels rapidly gel within a few minutes upon administration and exhibit robust rheological properties, excellent transparency, and negligible swelling/deswelling behavior. The hydrogel's biocompatibility and capacity to support cell growth were assessed using primary human corneal epithelial cells. Re-epithelialization on the NCColHA hydrogel was clearly observed in rabbit eyes, both *ex vivo* and *in vivo*, with expression of normal epithelial biomarkers, including CD44, CK12, CK14, α-SMA, Tuj-1, and ZO-1, and stratified, multilayered morphology. The applied hydrogel maintained its structural integrity for at least 14 days and remodeled into a transparent stroma by 56 days.**

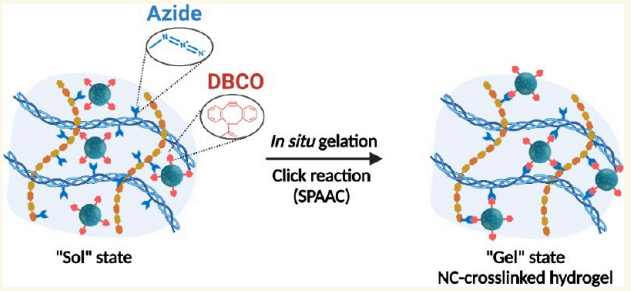

KEYWORDS: *bioorthogonal nanoclusters, bioorthogonally cross-linked hydrogel, corneal regeneration, corneal remodeling, scarless wound healing, structural integrity*

Inadequate healing of the cornea can lead to persistent epithelial defects, irregular astigmatism, progressive thinning, scarring, and possible perforation leading to severe vision loss.[1−3] A promising approach to promote corneal regeneration involves the application of *in situ* forming hydrogels to stromal defects.[4] When applied to defects, in situ-forming hydrogels can facilitate the regeneration of corneal layers as well as protect the defects from exposure to deleterious exposures.[5,6] To be effective for corneal repair, *in situ*-forming hydrogels must meet certain criteria: they should be transparent, biocompatible, adhesive to native tissues, and structurally stable until the cornea is fully repaired.[4,7,8] One effective strategy involves the use of UV light for cross-linking of the hydrogel components,[7,9,10] but this approach comes with potential ocular toxicities caused by UV light exposure and the generation of nonspecific reactive species such as free radicals. Host−guest interactions are a promising option, but these interactions may lack strong mechanical properties as they are reversible.[11] Alternatively, a number of non-photochemical reactions can also be employed to cross-link the components of hydrogels into structurally sound networks.[12,13] Nonetheless, many cross-linking chemistries also have a limitation of nonspecific side reactions with biological molecules, which have the potential to cause further damage to the cells and tissue in the wound bed.

Received: February 19, 2024
Revised: May 28, 2024
Accepted: June 7, 2024
Published: August 6, 2024

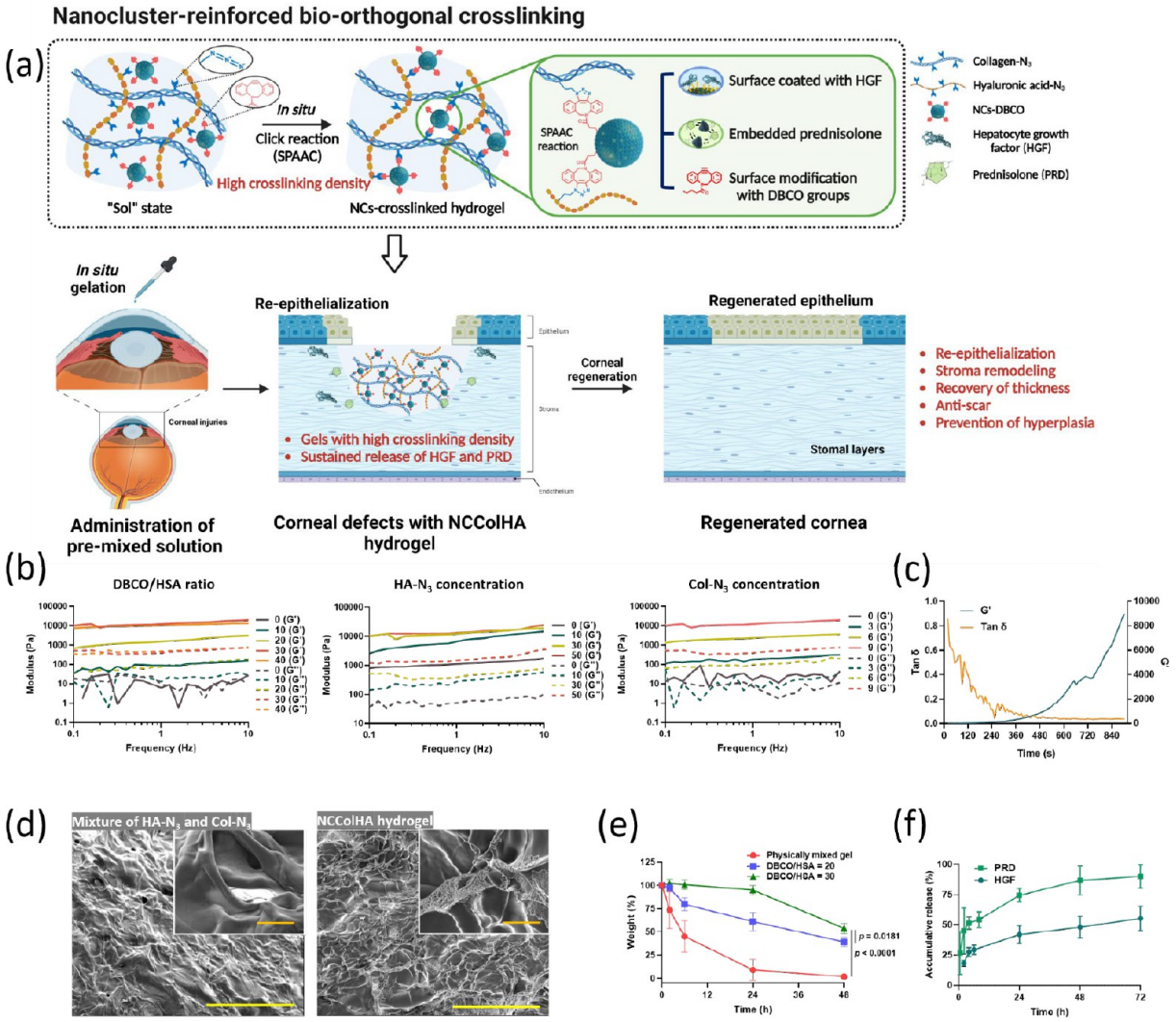

Figure 1. Characterization of the NCColHA hydrogel. (a) Schematic illustration for the application of NCColHA hydrogel. (b) Rheological properties of different NCColHA hydrogel formulations at 37 °C. The DBCO/HSA ratio indicates the molar ratio of DBCO to HSA when the concentrations of NCs, HA-N_3, and Col-N_3 were 40, 30, and 9 mg/mL, respectively. Hydrogels with varying concentrations of HA-N_3 were prepared at a constant concentration of NCs (40 mg/mL), Col-N_3 (9 mg/mL), and a DBCO/HSA ratio of 30. Hydrogels with different concentrations of Col-N_3 were prepared under the same conditions with concentrations of NCs (40 mg/mL), HA-N_3 (30 mg/mL), and a DBCO/HSA ratio of 30. (c) Changes in storage modulus and tan δ values over time. (d) SEM images of the surface of lyophilized NCColHA hydrogel (right) and a mixture of HA-N_3 and Col-N_3 without NCs (left). The length of yellow and orange scale bars is 100 and 10 μm, respectively. (e) Biodegradability assessment of NCColHA hydrogels with varying DBCO/HSA ratios in a solution containing ≥5 CDU/mL collagenase and 5 units/mL hyaluronidase. Physically mixed gel consisted of a mixture of the unmodified components. (f) Accumulative release patterns of HGF in a 1% BSA solution and PRD in 0.1% EtOH solution.

Bioorthogonal crosslinking reactions are promising for approaches to enhancing selectivity and biosafety, primarily due to their lack of cross-reactivity with cells, proteins, and glycosaminoglycans.[14] These hydrogels employ unique chemical reactions for cross-linking, such as nitrile oxide-norbornene cycloaddition[15] and strain-promoted azide−alkyne cycloaddition (SPAAC).[16,17] Many bioorthogonal reactions exhibit a time-course for gelation ranging from just a few minutes to several hundred minutes,[18] and those on the shorter end of that spectrum would be well-suited for *in situ* applications. We previously reported on bioorthogonally cross-linked hydrogels of collagen and hyaluronic acid that support robust epithelialization *in vivo*.[19,20] In this work, we build upon these studies to develop an *in situ* forming, bioorthogonally cross-linked hydrogel with substantially higher robust mechanical properties that is also engineered as a drug delivery platform that has the capacity to encapsulate two forms of therapeutic cargo, one with proregenerative effects (HGF) and one with anti-inflammatory effects (prednisolone)

Nanoparticle-cross-linked hydrogels have emerged as a promising strategy for drug delivery and tissue engineering.[21−25] Nanoparticles can serve as cross-linking nodes that improve the mechanical properties of hydrogels.[26] The large surface area and size of nanoparticles might contribute to effective conjugation with branches of hydrogel, conferring potential benefits such as controllable drug release and solubilizing effects.[27] However, this strategy can be applicable to only a limited range of nanomaterials because the cross-linking density depends mainly on physicochemical properties of nanoparticles, such as hydrophilicity, colloidal stability, the degree of substitution, intermolecular interactions with the frameworks of hydrogels, and the types of chemical reactions

https://doi.org/10.1021/acsnano.4c02345
ACS Nano 2024, 18, 21925−21938

involved.[17,27] Additionally, nanoparticle-cross-linked hydrogels for ocular applications have additional restrictions, as they must be transparent and free of color.

Here, we engineered a bioorthogonally cross-linked hydrogel reinforced with covalently bound nanoclusters loaded with therapeutic cargo for the purpose of facilitating the regeneration of injured corneal tissue (Figure 1a). Human serum albumin (HSA) was chosen as the nanocluster material due to the excellent water solubility, transparency, and drug loading capacity.[28,29] The surface of the NCs was decorated with dibenzocyclooctyne (DBCO) through covalent bioconjugation. In addition to cross-linking, we assessed the functions of NCs as a delivery platform by incorporating into them prednisolone acetate (PRD) and hepatocyte growth factor (HGF) as a model small molecule drug drug and model growth factor, respectively. For the hydrogel backbones, azide-modified hyaluronic acid (HA-N_3) and collagen (Col-N_3) were synthesized. Each component (i.e., NCs-DBCO, HA-N_3, and Col-N_3) was solubilized into separate solutions before being mixed, after which they became a rigid and transparent hydrogel within a couple of minutes. In this study, we assessed the physicochemical properties, transparency, and swelling/deswelling properties of NCColHA as well as its biocompatibility and ability to support corneal tissue regeneration both *in vitro* and *in vivo*.

RESULTS AND DISCUSSION

Design and Characterization. Albumin NCs were employed as a bioorthogonal cross-linker for the *in situ* forming hydrogel because of the protein's optical clarity in solution, biocompatibility, negative surface charge, and hydrophilicity, which were sufficient to maintain their solubility upon decoration with hydrophobic DBCOs. Moreover, previous research demonstrated that the NCs can encapsulate hydrophobic drugs within their structures and release the drugs slowly.[28] We leveraged these properties to design a dual-release system for the release of drugs and growth factors. In this research, PRD and HGF were employed as model hydrophobic drug and growth factor, respectively. PRD-embedded NCs were fabricated by modified ball-milling technology (BMT).[28,29] The surface of the NCs (40 mg/mL) was decorated with DBCO via primary amine/*N*-hydroxysuccinimide (NHS) reaction. When the NCs-DBCO were synthesized at a DBCO-to-HSA ratio of 30, the degree of substitution (DoS) was calculated as 35.5 ± 0.8% (Table S1). The high DoS is advantageous compared to previously reported DBCO-conjugated biopolymers (1.125−13%).[19,30,31] The substitution is limited due to the extremely hydrophobic properties of the DBCO moiety, which can cause the conjugated polymers to become unstable or precipitate. The hydrophilic nature of NCs offsets the hydrophobicity, and this high DoS would contribute to cross-linking density.[32] After the residual NHS esters were reacted, the NCs were coated with HGF through electrostatic interactions. The fabricated NCs exhibited a reversible aggregation/dissociation pattern and increased the apparent water solubility of PRD (Figure S1). As counter parts to DBCO, azide-conjugated hyaluronic acid (HA-N_3; 30 mg/mL) and collagen (Col-N_3; 9 mg/mL) were synthesized via primary amine/NHS reaction. The degree of substitution (DoS) values for HA-N_3 and Col-N_3 were calculated as 57.8 ± 0.9 and 50.9 ± 6.4%, respectively (Table S1). Hydrogels were fabricated by physically mixing equal volumes of each component. The refractive index of the NCColHA hydrogel was measured as 1.3355 ± 0.0001 (Table S2).

Hydrogels require robust mechanical strength to maintain their structure during wound healing processes.[33] To optimize the fabrication conditions, we prepared various hydrogels by altering three different factors: the molar ratio of DBCO to HSA and the concentrations of HA-N_3 and Col-N_3. The hydrogels exhibited distinct rheological properties based on the conditions (Figure 1b). The storage modulus values of the hydrogels increased as the molar ratio of DBCO to HSA increased from 0 (i.e., no bioconjugation) to 30. This confirms that DBCO was successfully conjugated to the NCs and that cross-linking occurred between the NCs and the azide-modified biopolymers. As further increasing the DBCO-to-HSA molar ratio to 40 did not further increase the storage modulus, we selected the DBCO-to-HSA ratio to be 30 for all future experiments. As expected, the quantity of HA-N_3 and Col-N_3 also influenced the mechanical properties. Storage modulus values generally increased as the amount of polymers increased, although no further increase was observed for HA-N_3 concentrations above 30 mg/mL. Therefore, we selected the concentrations of HA-N_3 and Col-N_3 as 30 and 9 mg/mL, respectively. Finally, we prepared the designed hydrogel (NCColHA hydrogel) by equally mixing NCs-DBCO (40 mg/mL; DBCO to HSA = 30), HA-N_3 (30 mg/mL), and Col-N_3 (9 mg/mL) in a 1:1:1 ratio (v/v/v). The fabricated hydrogel exhibited a G' value of over 20,000 Pa, which was almost 10 times higher than our previously developed bioorthogonal hydrogels.[19,20] This cross-linking process is safer and more efficient than other reported hydrogels.[7,9,34] Previously reported hydrogels for corneal defects have used external stimuli for cross-linking, such as UV and visible light, which typically in combination with an initiator result in the generation of reactive species that often lead to nonspecific byproducts. The use of bioorthogonal reactions for cross-linking has the advantage of not requiring an external trigger such as light and a high degree of specificity to avoid chemical reactivity with the biomolecules and cells within the wound bed, which is expected to mitigate further inflammation. NCColHA hydrogel exhibited a 3.56-fold higher compressive stress (2.46 MPa) than physical hydrogel (0.69 MPa), the result of greater mechanical strength by cross-linking (Figure S2).

The gelation of the mixture was assessed by measuring the storage modulus and tan δ values over time (Figure 1c). Initially, the storage modulus value was less than 20, and its tan δ value was 0.86, indicating a viscous solution state and partial gelation. Interestingly, the modulus values increased significantly over time, and the tan δ value dropped to less than 0.1 within 5 min, suggesting that the mixture underwent gelation.[35] Thus, gelation of the mixture occurs in a time-dependent manner. The formation of chemical bonds between the conjugated azides and DBCOs was evaluated by analyzing the infrared spectra (Figure S3). The azide-conjugated HA and Col exhibited an absorbance at approximately 2100 cm^{-1} (N═N═N), and DBCO-conjugated NCs also displayed an absorbance in a similar range (2050−2150; C≡C). In contrast, the NCColHA hydrogel displayed negligible absorbance at these ranges, which could be explained by depletion of azides and DBCO resulting from the click reaction.

The co-localization of NCs and polymer chains was observed using scanning electron microscopy (SEM) (Figure

https://doi.org/10.1021/acsnano.4c02345
ACS Nano 2024, 18, 21925−21938

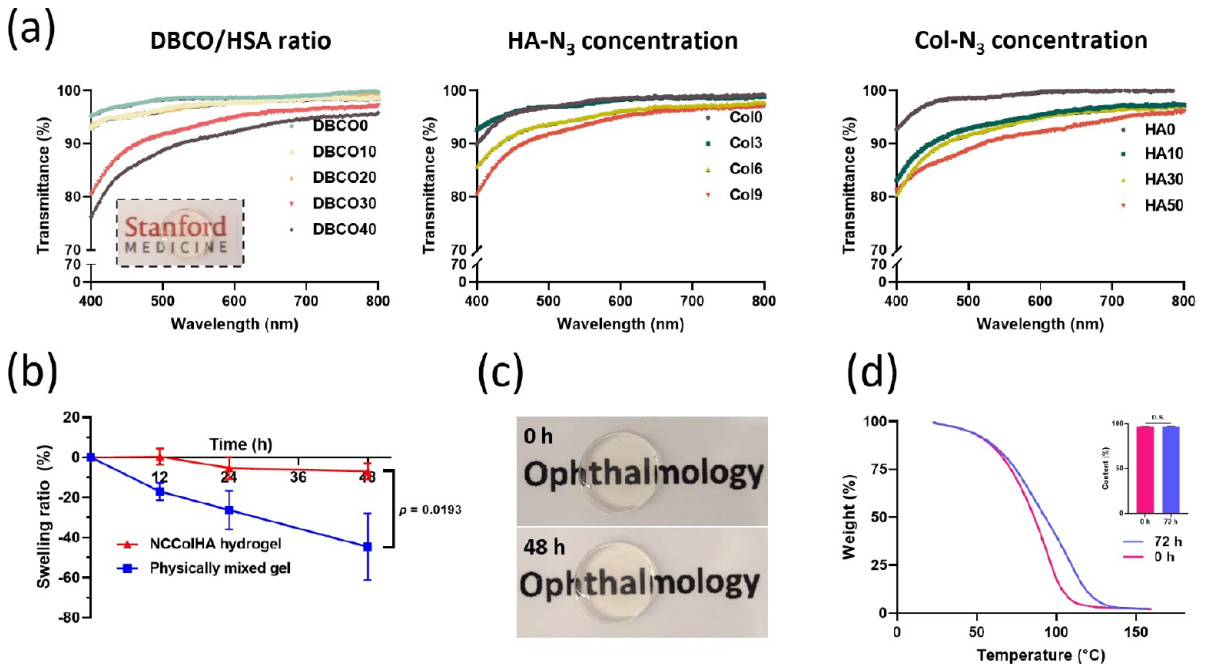

Figure 2. Transparency and swelling behavior of the NCColHA hydrogel. (a) Transmittance of different NCColHA hydrogel formulations. Transmittance of visible light ranging from 400 to 800 nm was measured. The dotted square image indicates the hydrogel placed over a background image. (b) The swelling ratio of NCColHA hydrogel in PBS at 37 °C. The physically mixed gel consisted of a mixture of the unmodified components. (c) Digital images of NCColHA hydrogel on a lettered background preincubation and postincubation for 48 h in PBS at 37 °C. (d) TGA analysis of NCColHA hydrogel preincubation and postincubation for 72 h in PBS at 37 °C. The inserted bar chart indicates the water content of hydrogel components (w/w). n.s.: not significant.

1d and Figure S4). NCColHA hydrogel was lyophilized, and the surface was observed to investigate the localization of NCs. Notably, the lyophilized NCColHA displayed a bundle of distinct aggregates embedded within the polymer, while these structures were not observed in a mixture of HA-N_3 and Col-N_3. The structure of the aggregates was more clearly observed with higher magnification (Figure S4). The sphere-shaped NCs appear similar to our previously reported albumin nanoclusters.[28] Their shapes can be variable, depending on the degree of chemical reactions with polymers (i.e., click reaction), because the NCs themselves are reversible clusters of drug-loaded albumin molecules. Therefore, these aggregate-bound branches were believed to result from NCs chemically bound to polymer chains, and the polar localization of NCs alongside the chains may imply chemical reactions between the components.

Biodegradability of the NCColHA hydrogel was assessed in a simulated body fluid solution containing 5 units/mL hyaluronidase and ≥5 CDU/mL collagenase (Figure 1e). The NCColHA hydrogel maintained more than 90% of its weight for 24 h, and 50% for 48 h. These values were significantly greater than those of the physically mixed hydrogel (i.e., a mixture of unmodified Col, HA, and NCs). Furthermore, its structural integrity decreased when the DBCO/HSA ratio was decreased to 20. These results suggest that the degree of cross-linking by NC-induced click reaction resulted in increased stability and slower biodegradability.

The release kinetics of PRD and HGF in physiological conditions were observed for 72 h (Figure 1f). In our design, PRD was embedded into NCs through hydrophobic interactions, and HGF was coated on the surface of NCs through electrostatic interactions. Both compounds were released continuously and slowly from the hydrogel, exhibiting sustained release patterns.[36] These patterns can be attributed to the noncovalent molecular interactions including hydrophobic and electrostatic interactions, as well as steric hindrances by the three-dimensional network of hydrogel.[37]

Transparency. Hydrogels for corneal administration must be transparent to avoid interference with clear vision. Hence, we assessed the transparency of the hydrogels by measuring the transmittance of visible light. The fabricated NCColHA hydrogel appeared highly transparent, allowing for a clear view of the background image (Figure 2a) and transmittance values with various conditions were measured in the visible light spectrum spanning 400 to 800 nm (Figure 2a). The optimized NCColHA hydrogel exhibited transmittance values consistently exceeding 80% across the entire wavelength range, indicating excellent transparency.[38] Of note, transmittance slightly decreased with an increase in DBCO-to-HSA ratio as well as with higher concentrations of HA-N_3 and Col-N_3.

Swelling and Deswelling Behavior. Swelling and deswelling are common phenomena observed in hydrogels,[39] but these characteristics are undesirable for hydrogels used in corneal defects. Ideally, the hydrogel should conform to the corneal defect and maintain its structural integrity and the as-formed dimensions. To evaluate the swelling/deswelling behaviors of NCColHA hydrogel, we first measured the weight change of the hydrogel after incubation in phosphate buffered saline (PBS) (Figure 2b). Interestingly, the NCColHA hydrogel exhibited minimal shrinking, with only a 7% reduction in weight after 48 h, while the physically mixed hydrogel (i.e., a mixture of the unmodified components; HA, Col, and NCs) experienced a significant weight loss of 44.6% over the same period. This suggests that cross-linking by NCs mitigates deswelling behavior. Figure 2c displays the appearance of NCColHA hydrogel before and after a 48 h

https://doi.org/10.1021/acsnano.4c02345
ACS Nano 2024, 18, 21925−21938

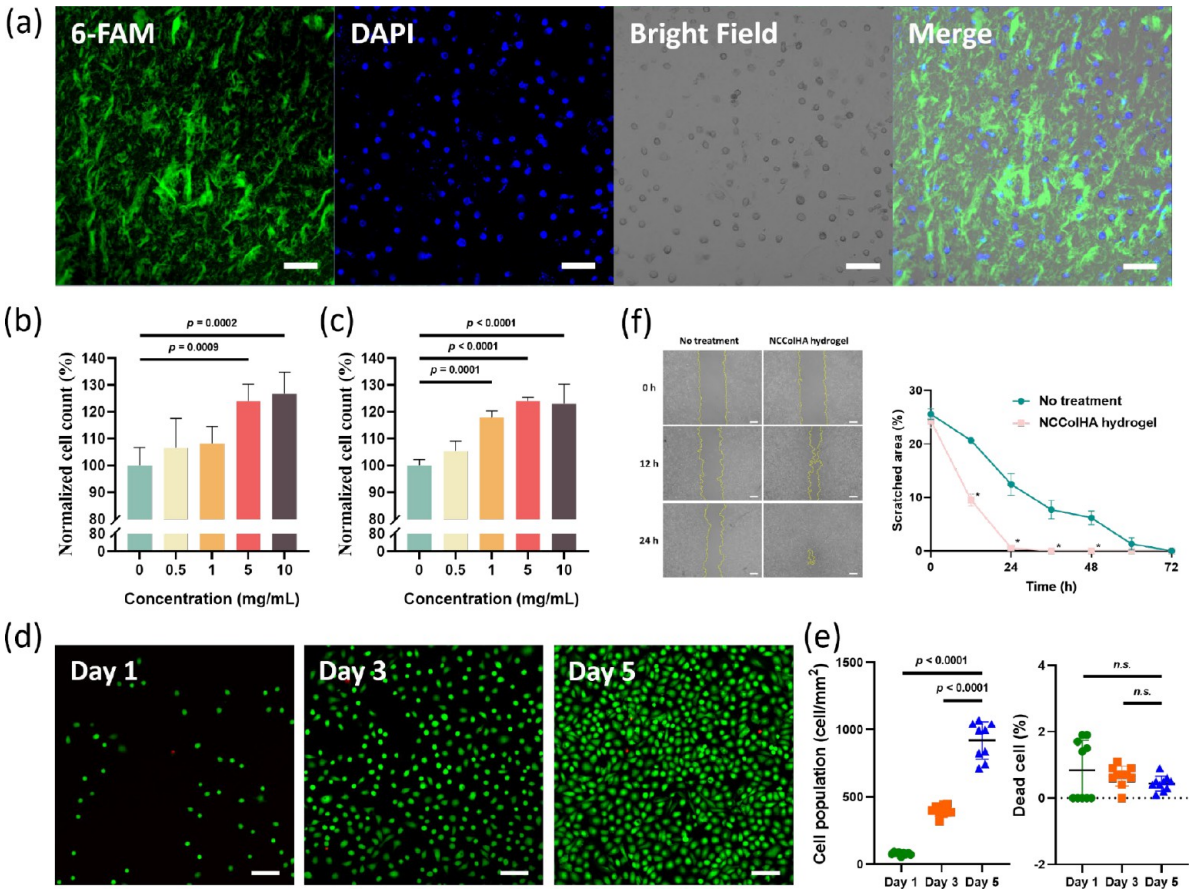

Figure 3. Cell compatibility and *in vitro* cell proliferation. (a) Confocal microscopic images of cells growing on the 6-FAM-labeled NCColHA hydrogel. The NCColHA hydrogel was spread on the culture dishes, and then, CECs were seeded on the hydrogel-coated surface. The cells were incubated for 2 days. The green, blue, and gray colors indicate 6-FAM, DAPI, and bright field, respectively. The scale bar length is 100 μm. Cell proliferation studies (b) when the cells were cultured in NCColHA-preadded condition (n = 5) and (c) when the NCColHA hydrogel was added to the cells after 1 day of incubation (n = 4). The x-axis represents the concentrations of the NCColHA hydrogels. Cell count was measured using CCK-8. (d) Live and dead cell analysis when the cells were cultured on the NCColHA hydrogel. The green and red colors indicate live and dead cells, respectively. The scale bar length is 100 μm. (e) The cell counts of live and dead cells observed in panel d (n = 9). (f) Cell migration assay when the cells were treated with NCColHA hydrogel (n = 3). The yellow dotted lines indicate the borders of the cells. The scale bar length is 400 μm. *n.s.*: not significant. *p <0.005.

incubation in PBS. The size of the hydrogel appeared unchanged after incubation, consistent with the results of the swelling ratio. To further confirm these swelling/deswelling properties, the water content of NCColHA hydrogel was analyzed by thermogravimetric analysis (TGA) (Figure 2d). The water content of NCColHA hydrogel was measured as 96.8 ± 0.2%, and this value did not significantly differ after postincubation for 72 h (97.0 ± 0.3%), indicating negligible swelling and deswelling properties of NCColHA hydrogel.

***In vitro* Cell Proliferation and Migration.** The cytocompatibility of the NCColHA hydrogel was assessed by culturing corneal epithelial cells (CECs) on the hydrogel. The NCColHA hydrogel was labeled with 6-FAM to visualize the localization of the hydrogel and cells. The 6-FAM-labeled NCColHA hydrogel was spread on cell culture dishes, and then the cells were cultured on the hydrogel (Figure 3a). After 2 days of incubation, we observed that the cells had proliferated well on the hydrogel, as demonstrated by an increase in the number of nuclei (visualized by DAPI) observed on the 6-FAM-labeled hydrogel. Additionally, we did not observe any differences in cell population between the hydrogel-coated area and uncoated area, supporting cell compatibility (Figure S5). These results demonstrate that CECs can proliferate on the hydrogel, indicating excellent cytocompatibility. Furthermore, we found that each component of hydrogel (i.e., Col-N_3, HA-N_3, and NCs-DBCO) exhibited excellent cytocompatibility with CECs (Figure S6).

Cell proliferation following treatment with NCColHA hydrogel was evaluated using the cell counting kit-8 (CCK-8) assay (Figure 3b,c). NCColHA hydrogel was treated with CECs in two different ways: through preaddition and postaddition of NCColHA hydrogels, allowing the assessment of cell proliferation under different gelation conditions. In the preaddition study (Figure 3b), cells were initially seeded on top of the NCColHA hydrogel and incubated for 2 days (i.e., hydrogel application before cell adhesion). In the postaddition study (Figure 3c), hydrogels were added to one-day precultured cells and incubated for 2 days (i.e., hydrogel application after cell adhesion). In both conditions, the cell population increased in a concentration-dependent manner. Considering each gel component did not affect the cell proliferation (Figure S6), these growth patterns can be attributed to the the pro-regenerative effects of the HGF released from the hydrogel.[40] Interestingly, the differences in cell viabilities between the two conditions were not significant except for the 1 mg/mL concentration. These results suggest

https://doi.org/10.1021/acsnano.4c02345
ACS Nano 2024, 18, 21925−21938

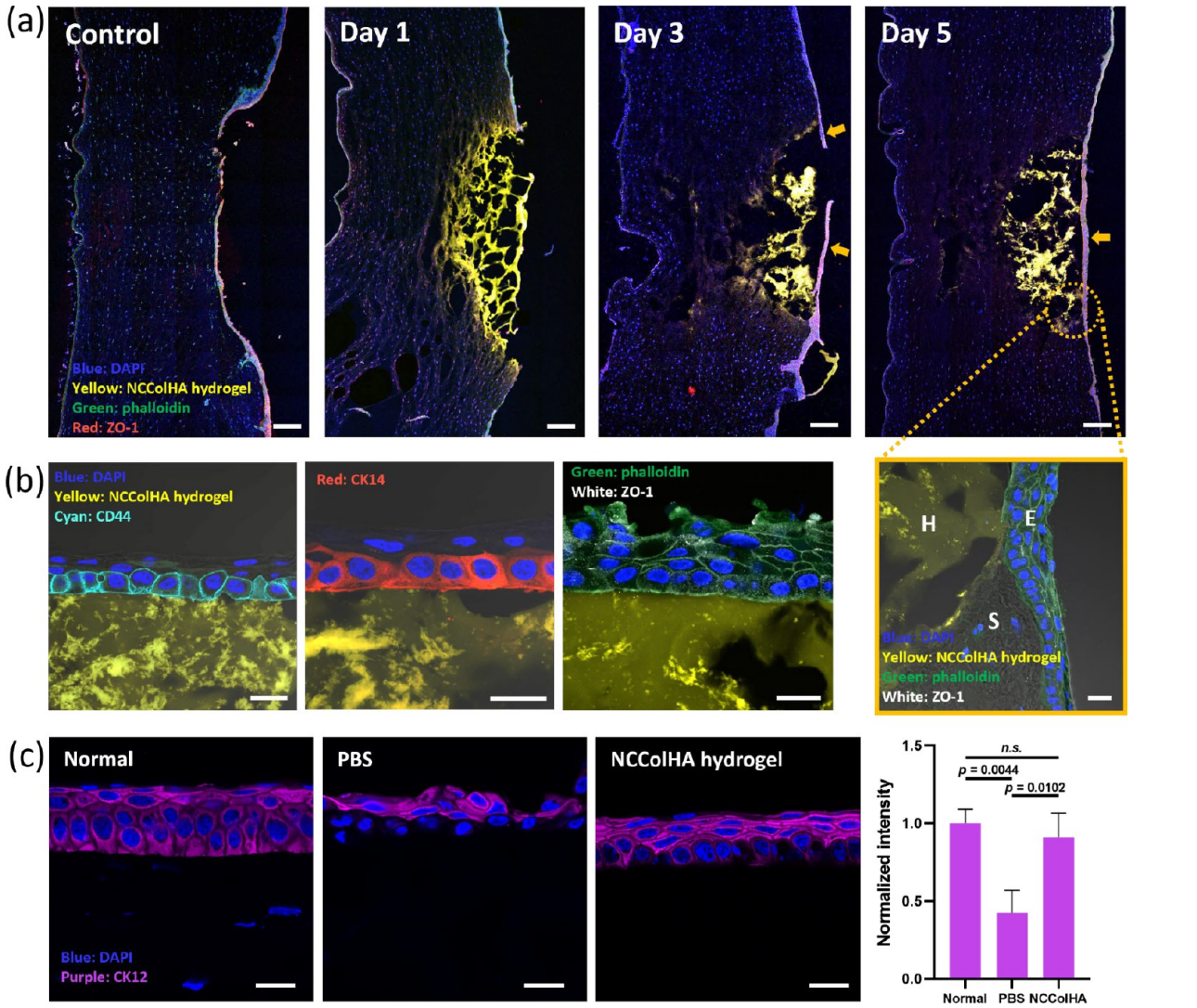

Figure 4. Immunohistochemistry of *ex vivo* rabbit cornea after treatment with the NCColHA hydrogel. (a) Entire corneal defects after administration of NCColHA hydrogel on days 1, 3, and 5. The control group indicates the corneal defects with PBS treatment on day 5. The orange arrows indicate the re-epithelialized layers on the hydrogel. The scale bar length is 200 μm. The magnified image indicates the edge of the corneal defect on day 5. H, E, and S indicate hydrogel, epithelial layer, and stroma, respectively. The scale bar length of the magnified image is 20 μm. (b) Epithelial biomarkers on day 5. The cyan, red, green, and white colors indicate the CD44, CK14, phalloidin, and ZO-1, respectively. The scale bar length is 20 μm. (c) CK12 expression in regenerated epithelial layers and its relative intensity (n = 4). The scale bar length is 20 μm.

that NCColHA hydrogel promoted cell proliferation regardless of the status of cellular adhesion.

We further confirmed cell proliferation and viability on the hydrogel. Epithelial cell proliferation on NCColHA hydrogel was evaluated by detecting live and dead cells over 5 days (Figure 3d,e). CECs were cultured on the hydrogel-coated surface, and the populations of live and dead cells were visualized using calcein-AM (green) and ethidium homodimer-1 (red), respectively (Figure 3d). The number of live cells significantly increased from day 1 to day 3 (5.01-fold) and from day 3 to day 5 (2.31-fold) (Figure 3e). Meanwhile, the percentages of dead cells remained below 2% through 5 days. Considering that the hydrogel is designed to support re-epithelialization *in vivo*,[19] these results suggest the high potential of the NCColHA hydrogel for corneal regeneration.

Epithelial cell migration from limbal stem cells across the cornea is a crucial process for regenerating and maintaining the epithelium,[40] and HGF has been shown to facilitate the motility of epithelial cells.[41] We assessed cell migration after incubating the cells with NCColHA hydrogels (Figure 3f and Figure S7). CECs were incubated until they reached a confluency of over 80%, and then a linear scratch was made in the middle of the cells to mimic a corneal epithelial wound. The initial scratched area was approximately 25% in both groups, and within 24 h, it decreased to 12.5 ± 2.0% in the untreated group. The scratch was completely closed in 72 h. In contrast, the cells treated with NCColHA hydrogel displayed a significantly faster closure of the scratched area within 24 h (0.6 ± 0.1%), indicating enhanced cell proliferation and migration.

Re-epithelialization of *Ex Vivo* Rabbit Corneas. Re-epithelialization in corneal defects is a pivotal process for wound closure to prevent bacterial infection, perforation, and scarring.[42] Our hypothesis is that the NCColHA hydrogel can suturelessly fill corneal defects and that epithelial cells would proliferate on the outer surface of the hydrogel. To observe the

https://doi.org/10.1021/acsnano.4c02345
ACS Nano 2024, 18, 21925−21938

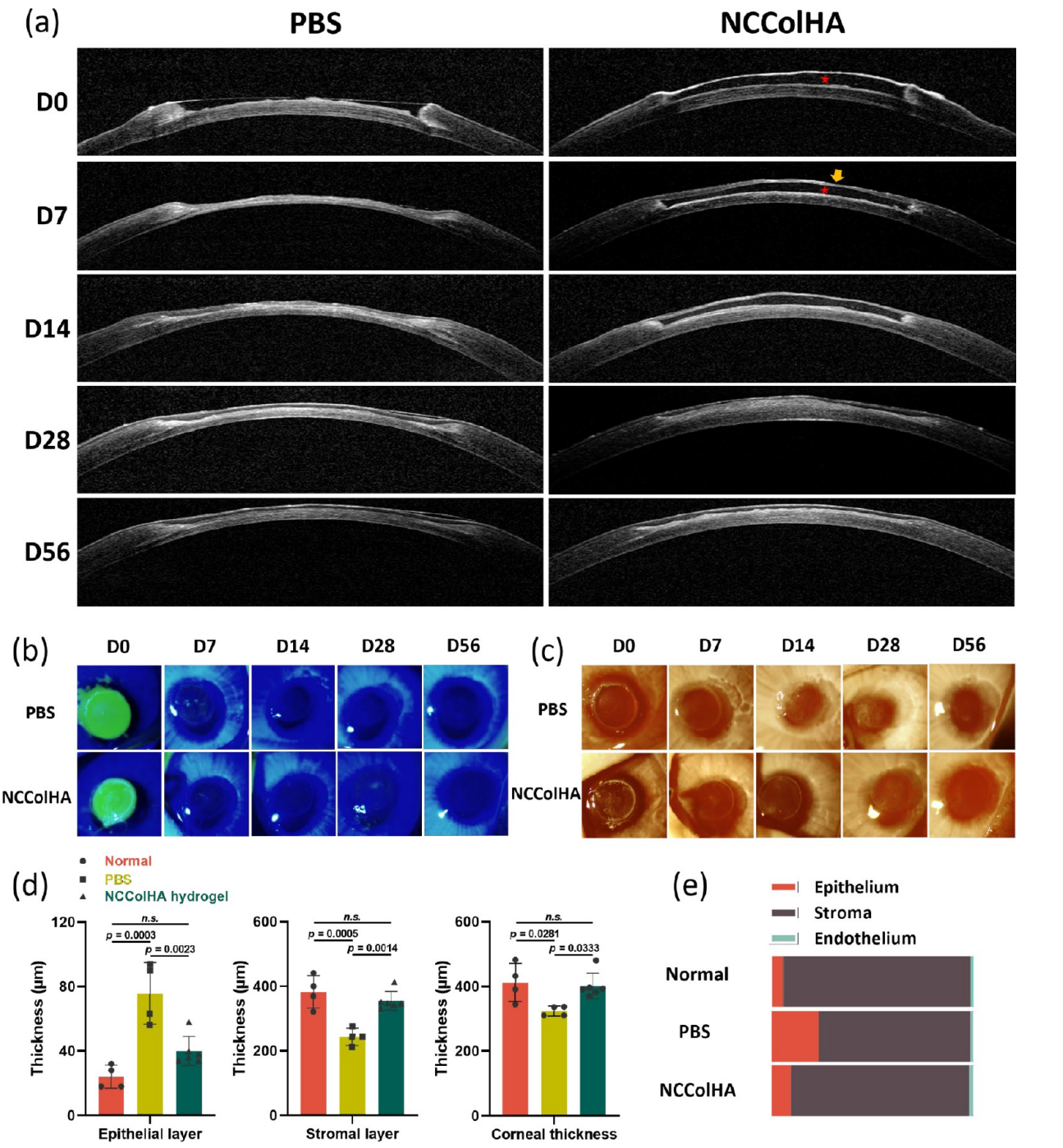

Figure 5. *In vivo* rabbit corneal wound healing studies ($n \geq 4$). (a) Representative OCT images of the keratectomized cornea after treatment with PBS only (left column) and the NCColHA hydrogel (right column). The red stars and orange arrows indicate the NCColHA hydrogel and regenerated epithelial layers, respectively. Images were taken on days 0, 7, 14, 28, and 56. (b) Representative photographs of the corneas after fluorescein staining intraoperatively and at each postoperative time point. (c) Representative digital slit lamp images of the corneas intraoperatively and at each postoperative time point. (d) Thicknesses of the regenerated epithelium, stroma, and whole cornea on day 56 ($n \geq 4$). (e) Graphical representation of the respective regenerated corneal layers 56 days after PBS versus NCColHA hydrogel treatment compared to normal corneas (scale of *x*-axis: 100%). n.s.: not significant.

re-epithelialization process, we used an *ex vivo* anterior lamellar keratoplasty (ALK) model using rabbit eyes.[43] Figure 4a shows keratectomy wounds treated with the NCColHA hydrogel. As shown in the control group (PBS-treated group; day 5), the cornea exhibited a distinct groove caused by defects, with re-epithelialization occurring within the groove. In contrast, in the cornea treated with the NCColHA, the hydrogels are seen filling the defects (yellow color; tagged with 6-FAM) with epithelialization (indicated by orange arrows) observed on their surface.

The structural integrity of the regenerated epithelial layer was assessed by observing the expression patterns of the epithelial biomarkers (Figure 4b,c). The corneal epithelium typically consists of five to seven cell layers, with the expression

https://doi.org/10.1021/acsnano.4c02345
ACS Nano 2024, 18, 21925−21938

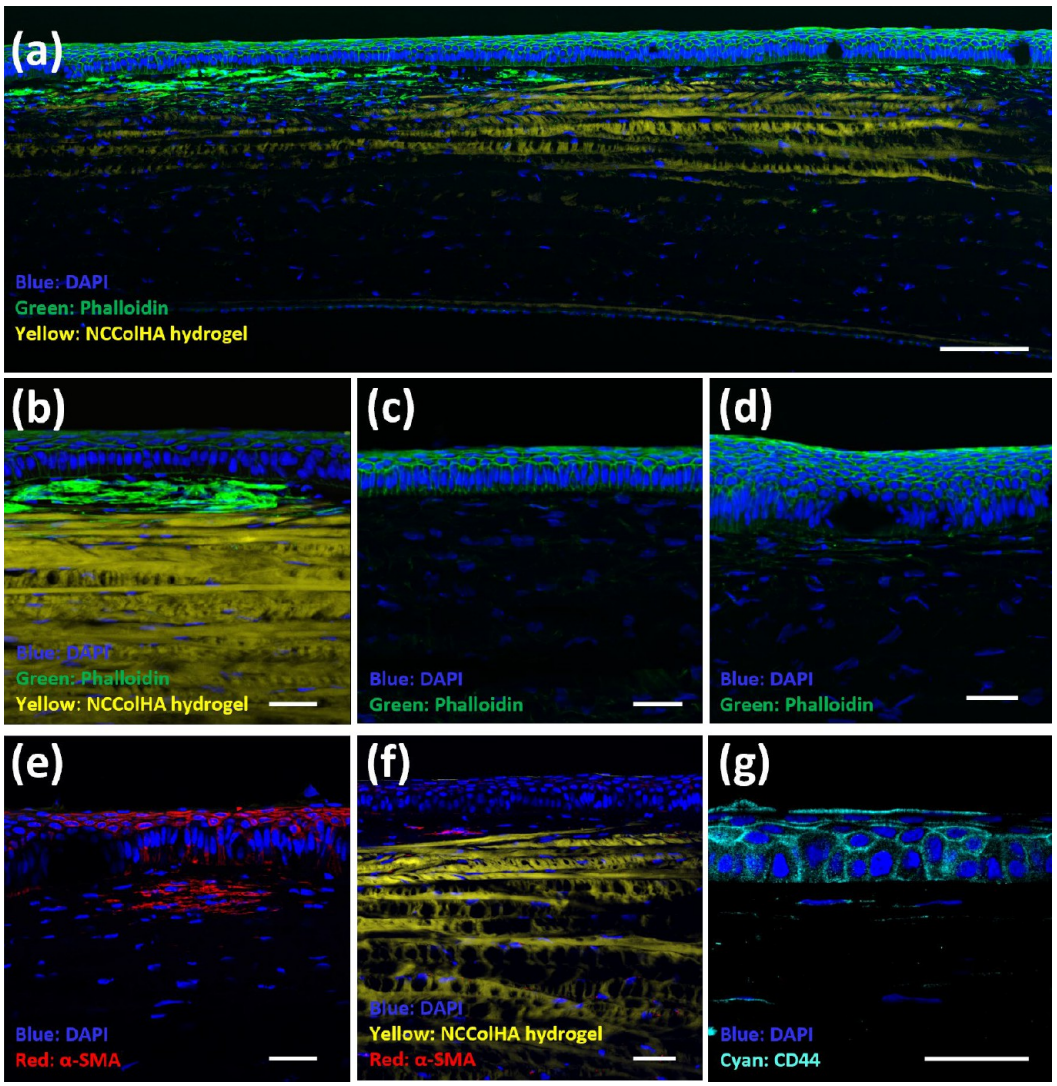

Figure 6. Immunohistochemical analysis of an *in vivo* rabbit cornea on day 56. (a) Wounded area of NCColHA hydrogel-treated cornea. The scale bar length is 200 μm. Epithelial layers of (b) NCColHA hydrogel-treated cornea, (c) normal cornea, and (d) PBS-treated cornea. α-SMA expression in the (e) PBS-treated cornea and (f) NCColHA hydrogel-treated cornea. (g) CD44 expression within the epithelium of the NCColHA hydrogel-treated cornea. The length of the scale bar in panels b–g is 40 μm.

of CD44 and CK14 being polarized in a basal layer.[44,45] CD44, a cell surface adhesion receptor, plays a role in cell-to-cell interactions crucial for corneal re-epithelialization,[44] providing adhesive strength to the epithelial layers. In addition to CD44, basal epithelial cells expressed cytokeratin-14 (CK14), suggesting limbal cell-like phenotype within the re-epithelialized layers.[45] CK14 is rarely expressed in normal central corneas but increases during corneal wound healing.[46−48] We found that the intensity of CK14 was significantly higher in the NCColHA hydrogel group than in the PBS group (Figure S8). To further assess the structural integrity of the stratified layers, we examined the formation of tight junctions (stained with ZO-1) between the cells.[49] Actin filaments within the cells were visualized using phalloidin (green), and nuclei were observed using DAPI (blue), while ZO-1 (white) delineated tight junctions between the cells. We also investigated the expression patterns of cytokeratin-12 (CK12), a cornea-specific differentiation biomarker, in the epithelia (Figure 4c).[50] This marker was expressed in all epithelial layers in the Normal and NCColHA groups, while the PBS group exhibited a polarized expression pattern in superficial layers, suggesting more complete cell differentiation in the NCColHA hydrogel group. All these epithelial biomarkers clearly indicate the structural integrity of the regenerated epithelial layers on the NCColHA hydrogel.

***In Vivo* Corneal Regeneration.** Corneal regeneration by the NCColHA hydrogel was also assessed in live rabbits (Figure 5). Corneal wounds were created using a 3.5 mm trephine to create anterior keratectomy wounds, and NCColHA hydrogel was applied to the defects (Figure S9). In this study, PBS-treated eyes were used as the control group. When treated with PBS, the re-epithelialization occurred within 1 week (Figure 5a), which is verified by fluorescein staining (Figure 5b). Then, the damaged stromal layers slowly recovered over 56 days. In contrast, in the NCColHA hydrogel group, the wounds were filled with the hydrogel (indicated by a red star) immediately after creation of the stromal defects. Notably, the applied hydrogels maintained their defect-filling structure for 14 days, and newly regenerated epithelial layers (indicated by an orange arrow) were clearly observed on the hydrogel. These results differ significantly from our previous work on a bioorthogonally cross-linked collagen-HA gel,[19]

https://doi.org/10.1021/acsnano.4c02345
ACS Nano 2024, 18, 21925−21938

where treated corneas were followed for 1 week and the gels were less clearly visible on OCT imaging but were visible upon immunohistochemical analysis. This difference in appearance on the OCT at 1 week may be attributed to the increased mechanical properties of the nanocluster-cross-linked hydrogel, which improves its resistance to dehydration and/or matrix turnover. Conventionally cross-linked hydrogels have exhibited low mechanical strength, high swelling ratio, fast biodegradability, and low adhesiveness, which may be attributed to fast clearance of hydrogels *in vivo*.[4,51−53] Clinical evidence of re-epithelialization was confirmed using fluorescein staining (Figure 5b). The epithelial layers of both the control and treated corneas were found to all be completely healed on day 7. We also monitored the transparency of the corneas each day (Figure 5c). The eyes of the PBS group had moderate-to-severe scars on days 14 and 28 and disappeared on day 56. In contrast, the NCColHA hydrogel group exhibited negligible opacities over the entire evaluation period. Whole OCT and digital slit lamp images are presented in Figure S10. We further evaluated the ratio of mean epithelial-to-stromal reflectivity (ES ratio) and found that the PBS group exhibited significantly lower values on days 28 and 56, while the NCColHA hydrogel group did not (Table S3). This suggests that the regeneration of stromal and epithelial layers with relative thicknesses closer to normal cornea was promoted when treated with NCColHA hydrogel.

The presence and appearance of the gel was monitored using OCT through 56 days after surgery and treatment. The NCColHA hydrogel appeared mostly intact through day 14 with a characteristic dark appearance throughout its bulk and a hyper-reflective surface, which we interpreted as the regrown epithelium. By day 28, the dark band appeared thinner, while the stromal bed appeared thicker with a thicker zone of hyperreflectivity anteriorly, appearing to now occupy the posterior interface of the hydrogel. By day 56, a thin, well-defined dark band remained, with a smooth overlying hyper-reflective band of epithelium and a more discrete band of hyperreflectivity posteriorly, with an overall more compact and smoother contour and uniformity across all layers.

To quantitatively analyze corneal regeneration, the thicknesses of the treated and untreated (saline control) corneas were calculated and compared to that of normal (uninjured, untreated) corneas (Figure 5d and Figure S11). The thickness of the epithelium, stroma, and full thickness cornea in normal eyes ($n = 4$) was calculated as 24 ± 7, 383 ± 51, and 412 ± 59 μm, respectively. In the PBS-treated group, the thickness of the whole cornea slowly increased for 56 days, but it did not fully recover (323 ± 15 μm; $n = 4$) by 56 days, with a statistically significantly thicker epithelium (76 ± 19 μm) but thinner stroma (243 ± 27 μm) and overall thickness compared to normal corneas (Figure 5d). This observation is consistent with epithelial hyperplasia, which is a common observation during the regeneration after stromal injuries.[54,55] In contrast, the injured cornea exhibited significant regeneration when treated with NCColHA hydrogel, resulting in epithelial (40 ± 9 μm), stromal (355 ± 29 μm), and overall cornea thickness (402 ± 40 μm; $n = 6$) that were not statistically significantly different from the normal corneas at 56 days. The epithelial thickness in the NCColHA hydrogel group was also slightly increased (40 ± 9 μm) but was not statistically significantly different from that of normal corneas. NCColHA hydrogel groups exhibited a robust recovery of cornea structures, with components appearing similar to those of normal corneas (Figure 5e).

Immunohistochemical Analysis. The treated corneas at day 56 were further evaluated by immunohistochemical analysis (Figure 6) to visualize the hydrogel and markers of the corneal cell structure and function. Interestingly, Figure 6a shows a partially remodeled NCColHA hydrogel that is integrated with a newly formed host extracellular matrix, with host stromal cells and new collagen observed both within and alongside the hydrogel. This observation suggests that host corneal stromal cells are able to infiltrate and degrade the NCColHA matrix and lay down new extracellular matrix. Notably, F-actin was observed in the areas between the hydrogel and epithelium, indicating potential cell-matrix mechanical interactions at the wound site.[56] The NCColHA hydrogel-treated corneas exhibited a multilayered epithelium with a normal thickness (Figure 6b), similar to that of normal corneas (Figure 6c). In contrast, the PBS-treated cornea exhibited a significantly thicker epithelium (Figure 6d). In addition to this observed hyperplasia, we analyzed α-smooth muscle actin (α-SMA) expression at the wound site of the PBS-treated corneas, which is indicative of fibrotic healing (Figure 6e,f). In corneal wounds, activated keratocytes can differentiate into α-SMA-positive myofibroblasts, inducing scarring.[57] Notably, the corneas treated with the NCColHA hydrogel exhibited significantly reduced the expression of α-SMA compared to the PBS treatment, suggesting a reduction in myofibroblastic activity and fibrosis,[58] consistent with the relatively clear clinical appearance of the corneas with slit lamp photography (Figure 5c). CD44 expression further confirms the structural integrity and interaction of the regenerated epithelium with the NCColHA hydrogel (Figure 6g). We also investigated nerve regeneration in the healed cornea by staining for neuron-specific class III beta-tubulin (Tuj-1) (Figure S12).[59,60] In the stromal layers, the NCColHA hydrogel group exhibited no significant difference compared to the normal corneas, while the PBS group exhibited significantly lower stromal intensities for this marker than the other groups. This indicates that the NCColHA hydrogel promoted regrowth of corneal nerves—which had been removed at the time of the keratectomy—into the wound area. Additionally, the regenerated tissue anterior to the residual stromal bed in the NCColHA group exhibited no significant difference in the amount of collagen I compared with the normal group. Meanwhile, the PBS treatment group yielded a significantly thinner cornea and reduced overall collagen I content anterior to the residual stromal bed. Given that the NCColHA hydrogel has a relatively low content of collagen type I (0.3%, w/v) compared to natural corneal stroma, the collagen visualized by our immunohistochemical staining is likely to be predominantly newly formed collagen in the remodeled anterior stroma (Figure S13).

CONCLUSIONS

We have developed a bioorthogonally cross-linked, nanocluster-reinforced hydrogel for the regeneration of corneal defects. The nanoclusters (NCs) were composed of a composite of albumin and the steroid prednisolone bound together by hydrophobic interactions and were surface modified with strained alkyne (DBCO) groups via chemical linkages as well as the growth factor HGF by virtue of electrostatic interactions. These DBCO-decorated NCs react with azide-conjugated HA and Col to achieve rapid gelation

https://doi.org/10.1021/acsnano.4c02345
ACS Nano 2024, 18, 21925−21938

within a few minutes *in situ* within corneal defects through strain-promoted azide−alkyne cycloaddition (SPAAC), a bioorthogonal cross-linking reaction. The resulting NCColHA hydrogel exhibits excellent biocompatibility, mechanical properties, transparency, and negligible swelling/deswelling properties, creating an ideal substrate for corneal regeneration. In a rabbit corneal defect model, our study showed that the NCColHA hydrogel maintained its structural integrity for at least 14 days, facilitating re-epithelialization over the hydrogel. By 2 months, the corneas exhibited excellent transparency and hydrogel was partially remodeled without observable fibrosis and had integrated host stromal cells and extracellular matrix along with multilayered epithelialization resembling that of a normal cornea at 8 weeks post injury and treatment. Based on these findings, the NCColHA hydrogel developed and described herein appears to be a promising approach meriting further development and investigation for the treatment of deep stromal corneal defects.

MATERIALS AND METHODS

Materials. Human serum albumin (HSA), L-lysine, fluorescein, prednisolone (≥99%), and bovine serum albumin (BSA) were purchased from Sigma-Aldrich (St. Louis, MO, USA). Hyaluronic acid amine (MW 250k; DoS of 50%) was obtained from Creative PEGWorks (Durham, NC, USA). Collagen (TeloCol-10) was provided by Advanced BioMatrix (Carlsbad, CA, USA). DBCO-sulfo-NHS ester (99%) and Azido-PEG5-NHS ester (98%) were purchased from BroadPharm (San Diego, CA, USA). Recombinant human hepatocyte growth factor protein (HGF; active form) was purchased from Abcam (Cambridge, UK).

Fabrication of NCColHA Hydrogel. To fabricate the bioorthogonally cross-linked hydrogel, we prepared azide-conjugated HA (i.e., HA-N_3), azide-conjugated collagen (i.e., Col-N_3), and DBCO-decorated NCs (NCs-DBCO). For the synthesis of HA-N_3, the neutralized hyaluronic acid amine solution (HA-NH_2; 20 mg/mL) was prepared using 10X PBS and 1N NaOH. Meanwhile, the azido-PEG5-NHS ester solution was diluted with DMSO (dilution factor: 2). The azido-PEG-NHS ester solution (20.52 μL) was mixed with the HA-NH_2 solution (1 mL) and vortexed overnight under light-protected condition. Then, the product solution was dialyzed (MWCO = 12−14 kDa) against distilled water (DW) for 2 days. DW was replaced two times a day for 2 days. The dialyzed solution was lyophilized and stored at −20 °C until use.

Col-N_3 was prepared in the way like the HA-N_3. Collagen solution (9 mg/mL) was prepared by neutralizing with 10X PBS and 1N NaOH, and azido-PEG5-NHS ester was diluted 10 times with DMSO. The diluted azido-PEG5-NHS ester solution (20.7 μL) was added into the neutralized collagen solution (1 mL) and rotated gently at 4 °C overnight. The product solution was dialyzed against PBS using Slide-A-Lyzer G2 Dialysis Cassettes at 4 °C overnight.

For the fabrication of DBCO-decorated NCs, albumin-based NCs were fabricated by modifying the Ball-Milling Technology.[28,29] Briefly, HSA (20 mg) and prednisolone (PRD; 4 mg) were mixed, and 9.5% DMSO solution (in PBS; 4.75 μL) and stainless-steel beads (diameter: 5 mm; PGN Bearings) were added into the powder. Then, the mixture was vortexed for 10 min. The suspension was lyophilized to clearly remove the DMSO. The lyophilized powder was reconstituted using DW (0.4 mL) and centrifuged at 5000 rpm for 1 min. After that, the supernatant was filtrated using a syringe filter (0.45 μm) to eliminate the unbound prednisolone. For the decoration of DBCO on the surface of NCs (DBCO/HSA ratio = 30), a DBCO-sulfo-NHS ester solution was prepared in PBS (100 mg/mL) and added (19.2 μL) into the NC suspension (40 mg/mL). The suspension was gently rotated for 2 h under light-protected conditions. After incubation, L-lysine solution (140 mg/mL in PBS; 3.76 μL) was added to the suspension to inactivate the residual NHS ester, and the suspension was gently rotated for 30 min. Finally, an HGF solution (240 μg/mL in PBS; 2.5 μL) was added into the suspension to load the HGF on the surface of NCs. NCColHA hydrogel was prepared by mixing HA-N_3, Col-N_3, and NCs-DBCO in equivalent proportions (1:1:1, v/v/v).

Characterization. To investigate the rheological properties of NCColHA hydrogel according to different fabrication conditions, we prepared five kinds of NCs-DBCOs (DBCO/HSA ratio = 0, 10, 20, 30, and 40), four kinds of HA-N_3 solutions (concentrations of 10, 30, and 50 mg/mL), and three types of Col-N_3 (concentrations of 3, 6, and 9 mg/mL). The storage and loss modulus of each gel were measured by a rheometer (ARES-G2; TA Instruments, New Castle, DE, USA) at frequencies ranging from 0.1 to 10 at the oscillation strain of 1 at 37 °C. The change of storage modulus and tan δ values over time was measured at the oscillation strain of 1% at 37 °C. The tan δ value was defined as loss modulus (G'')/storage modulus (G'). The infrared spectra of NCColHA hydrogel and each component were obtained by a Fourier-transform infrared spectrometer (Nicolet iS50; Thermo Fisher Scientific; Waltham, MA, USA). The hydrogel was lyophilized, and the hydrogel powder was analyzed by an FT-IR spectrometer. The SEM images (Thermo Fisher Scientific Apreo S LoVac Scanning Electron Microscope) were obtained by observing the surface of the lyophilized hydrogel. In this observation, a mixture of HA-N_3 and Col-N_3 was also prepared to compare the microstructures.

Biodegradability. Biodegradability of NCColHA hydrogel was investigated against three kinds of NCColHA hydrogels according to the DBCO/HSA ratio (20, 30, and 40). In this study, the unmodified hydrogel (i.e., physical mixture of HA-NH_2, collagen, and NCs) was employed as a control. The initial hydrogels were weighed (W1), and they were submerged in the mixture of 5 units/mL hyaluronidase (Sigma-Aldrich) and ≥5 CDU/mL collagenase (Sigma-Aldrich). The hydrogels were incubated at 37 °C. The weight of the hydrogels (W_n) was measured at 2, 6, 24, and 48 h. The percent weight (%) of the hydrogels at those points was calculated as $W_n/W_1 \times 100$.

***In Vitro* HGF and PRD Release.** The release patterns of HGF and PRD from the NCColHA hydrogel were evaluated in 0.1% EtOH (PRD) or 1% BSA (HGF) solution. To calculate the amount of PRD embedded in the NCs, PRD was extracted using ACN (dilution factor: 10) and centrifuged (14,000 rpm, 5 min). The supernatant was further diluted with DW, and the absorbance at 245 nm was analyzed with a microplate reader (TECAN, Männedorf, Switzerland). The release kinetics of PRD was investigated in 0.1% EtOH solution (in PBS). NCColHA hydrogel was inserted into the dialysis membrane tubing (6−8 kDa) and incubated with gentle shaking. The release profile of HGF was assessed in 1% BSA solution without using the dialysis bag. The hydrogel was pregelated, and the release medium was added. The amount of released HGF was calculated using a human HGF ELISA kit (Abcam).

Transparency. To visualize the transparency of the NCColHA hydrogel, the fabricated hydrogel was put on a plastic card with lettering in the background, and photos were taken by focusing on the background letters. In addition to the visual images, transparency was quantified by measuring the transmittance of visible light spectrum from 400 to 800 nm. The percentage of transmittance was calculated for each hydrogel in comparison with that of PBS.

Swelling Ratio. Swelling property of NCColHA hydrogel was assessed by measuring the weight of hydrogel after incubated in PBS at 37 °C. Briefly, the weight of hydrogel was measured prior to incubation (W_0), as well as at 12, 24, and 48 h postincubation (W_n). The swelling ratio was calculated as follows: $(W_n - W_0)/W_0 \times 100$. The digital images of the NCColHA hydrogel were also taken before and after incubation for 48 h. To compare the size difference after incubation, the hydrogel was placed on a plastic card with a lettering background. To confirm the swelling property, the contents of NCColHA hydrogel were measured by a thermogravimetric analyzer (TGA; TA Instruments, DE, USA). The NCColHA hydrogel was incubated in PBS for 72 h, and its thermogravimetric pattern was subsequently compared with that of the hydrogel at the initial point (0 h).

https://doi.org/10.1021/acsnano.4c02345
ACS Nano 2024, 18, 21925−21938

Cell Culture. Corneal epithelial cells (CEC; ATCC; CRL-11135) were cultured to test the cell proliferation and cytotoxicity. Cells were cultured in a keratinocyte-serum-free medium supplemented with a 5 ng/mL epidermal growth factor, 500 ng/mL hydrocortisone, 0.05 mg/mL bovine pituitary extract, and 5 μg/mL insulin. Cells were incubated at 37 °C in a 5% CO2 atm, and the medium was refreshed every other day. The proliferated cells were passaged at 80% confluency using a Trypsin-EDTA solution.

Cell Compatibility. To investigate the cell compatibility of the NCColHA hydrogel to the CECs, the NCColHA hydrogel was thinly spread on the ground of culture dishes, and cells (4×10^4 cells) were seeded on the dishes. To visualize the hydrogel on the ground, Col-N_3 was labeled with 6-FAM NHS ester (Lumiprobe, Maryland, USA). Briefly, FAM NHS ester solution (2 μL; 7.1 mg/mL in DMSO) was added to Col-N_3 solution (100 μL) and incubated overnight at 4 °C under light-protected conditions. The cells were incubated for 2 days. After being incubated, the cells were stained with DAPI solution, and their fluorescents were observed using a confocal microscope (Carl Zeiss, Oberkochen, Germany). The cell morphology on the gel was also investigated by using an optical microscope.

Cell Proliferation Study. To evaluate the cell count of CECs when treated with NCColHA hydrogel, the cells (1×10^4 cells) were seeded on 96 well culture plates and incubated for 1 day prior to treatment. Then, the NCColHA hydrogel was treated to the cells at five different concentrations of NCColHA hydrogel (0, 0.5, 1, 5, and 10 mg/mL). The samples were prepared in two different ways. One is that the cells were cultured in NCColHA hydrogel-preadded condition. The other is that NCColHA hydrogel was added to the preincubated cells. All the treated cells were incubated for 2 days, and their cell population was analyzed using Cell Counting Kit-8 (CCK-8; Dojindo Molecular Technologies, MD, USA). After incubating with CCK-8 solution for 2 h, the absorbance (450 nm) of the supernatant was analyzed with a microplate reader.

Cell proliferation on the NCColHA hydrogel-coated ground was assessed by measuring the cell populations and the ratio of dead cells. NCColHA hydrogel was coated on the culture flask in the same way as for the compatibility study. Then, CECs (3.5×10^5 cells) were seeded on the hydrogel and incubated for 5 days. The cell proliferation was assessed by monitoring the cell populations on days 1, 3, and 5. The live and dead cells were detected using a Live/Dead Viability/Cytotoxicity Kit (Invitrogen, MA, USA). The cell number of each image was measured by using ImageJ software.

Cell Migration Assay. To make the artificial wounds, the Parafilm piece (1.6 mm × 5.0 mm) was stuck to the ground of cell culture dishes (100 mm). These dishes were sterilized using 70% ethanol and ultraviolet (UV) light irradiation. CECs (1×10^5 cells in 10 mL of cell culture medium) were seeded on the dishes and incubated until the cells were fully proliferated. Then, the Parafilm was removed to make the artificial wounds, and the NCColHA hydrogel (100 μL) was added alongside the wounds. The wounds were monitored using an optical microscope at every 12 h up to 72 h.

***Ex Vivo* Wound Healing Study.** The wound healing processes after application of hydrogel were assessed using an *ex vivo* rabbit eye culture model. Briefly, a lamellar keratectomy with a 3.5 mm trephine (Robbins Instruments, CA, USA) was carried out on the rabbit corneas. The defected corneas were cut off from the eyes leaving a 5 mm thick ring of sclera, removing lens and iris. The corneas were washed two times with 1% penicillin-streptomycin (PS) solution. The corneas were then mounted on agar plugs. The agar plugs were prepared by microwaving 2 g of agar in 75 mL of organ culture medium containing DMEM/F12 (Gibco, MT, USA), insulin-transferrin-selenium (0.05%), and PS (1%). The agar was solidified using a PDMS mold, and the obtained rabbit cornea was placed on the agar plugs. Ater mounting the corneas, the culture medium was added until it met the sclera. After that, 6-FAM-labeled NCColHA hydrogel was applied to the defects (3−5 μL) to fill out the defects and harvested on days 1, 3, and 5. The PBS-treated cornea was employed as a control group, and the control group was harvested just on day 5. The collected corneas were sliced for the analysis of immunohistochemistry.

Immunohistochemistry. To observe the morphologies and biomarkers in the hydrogel-treated areas, the corneas were sliced and stained using various kinds of antibodies. NCColHA hydrogel was labeled with 6-FAM as desribed above. For *ex vivo* analysis, the slices were stained with DAPI (1:1000, Thermo Fisher Scientific), anticytokeratin 12 (anti-CK12; 1:100, Abcam), anticytokeratin 14 (anti-CK14; 1:100, Abcam), anti-CD44 (1:100, Abcam), anti-ZO-1 (1:100, Invitrogen), and Alexa fluor 647-conjugated antiphalloidin (1:400, Thermo Fisher Scientific). Subsequently, the anti-CK14, CD44, and ZO-1 antibodies were captured with Alexa fluor 555-conjugated antirabbit IgG (1:200, life technologies corporation, CA, USA), Alexa fluor 647-conjugated antirat IgG (1:200, life technologies corporation), and Alexa fluor 555-conjugated antimouse IgG (1:200, life technologies), respectively. The fluorescent signals from each sample were detected with a confocal microscope. For *in vivo* analysis, anti-α-smooth muscle actin (α-SMA; 1:500, Abcam) was primarily used, and Alexa fluor 647-conjugated antimouse IgG (1:200, life technologies corporation) was subsequently added for a secondary staining.

Animals. New Zealand white rabbits (3.5−5.5 kg) were used in this study. Animal experiments were designed to conform with the ARVO statement for the Use of Animals in Ophthalmic and Vision Research and were reviewed and approved by the Stanford University Institutional Animal Care and Use Committee (protocol #: APLAC-33413). All anesthesia procedures were supported by the veterinary service center (VSC) at Stanford University.

***In Vivo* Corneal Regeneration.** For all surgeries and follow-up studies, we dropped proparacaine hydrochloride ophthalmic solution (0.5%; Bausch and Lomb, Laval, Canada) to the eye that would be examined. To establish the corneal defect model, lamellar keratectomy was performed on one eye using a 3.5 mm trephine to create a deep circular cut (50−70% depth of corneas) and a spatula to remove the collagen fibril layers. After applying the mixture of each hydrogel component (i.e., the mixture of HA-N_3, Col-N_3, and NCs-DBCO; 1:1:1, v/v/v) on the artificial defects, we waited for 10 min for the gelation of the applied solution. Then, a contact lens was applied to protect the hydrogel from scratching or other stresses, and tarsorrhaphy was carried out to prevent agitation by the animal and to help keep the contact lens and gel in place. As a postoperative care, ofloxacin ophthalmic solution (0.3%, Bausch and Lomb) was added three times a day for 1 week to prevent the bacterial infection, and prednisolone acetate ophthalmic suspension (1%, Sandoz, Basel, Switzerland) was dropped three times a day for the day after surgery to relieve the initial inflammation caused by the lamellar keratectomy.

The corneal defects after application of the NCColHA hydrogel were monitored by taking optical coherence tomography (OCT; Heidelberg Engineering, Heidelberg, Germany) images and photographs. To check the re-epithelialization of the defected areas, fluorescein solution (1.5%) was dropped and washed immediately with the balanced salt solution (Alcon, Geneva, Switzerland). The fluorescein-stained areas were detected by using blue light. On day 7, the tarsorrhaphy was removed for eye examination, and the defects were further monitored on days 14, 28, and 56. The eyes were enucleated and cryo-sectioned for immunostaining after examination on day 56. The cornea slices were stained with DAPI, phalloidin, anti-CK14, and anti-α-smooth muscle actin (anti-α-SMA; Abcam). The thickness of the epithelial and stromal layers and whole cornea on day 56 was measured based on confocal microscopic images of the sliced sections.

Statistical Analysis. All the statistical analyses were performed using Graphpad Prism software (version 8.0.2.263). For multiple comparisons, we employed one-way ANOVA followed by Tukey's posthoc analysis. For pairwise comparisons, the significance was determined using a two-tailed unpaired t test. The significance threshold was set at $p < 0.05$; otherwise, the difference was labeled as "not significant (n.s.)".

https://doi.org/10.1021/acsnano.4c02345
ACS Nano 2024, 18, 21925−21938

ASSOCIATED CONTENT

Supporting Information

The Supporting Information is available free of charge at https://pubs.acs.org/doi/10.1021/acsnano.4c02345.

Degree of substitution (DoS) values of the synthesized materials; refractive index of NCColHA hydrogel and its components; epithelial-to-stromal reflectivity ratio (ES ratio) of rabbit eyes in *in vivo* study; characterization of NCs; compressive stress−strain curves of hydrogels; Fourier-transform infrared (FT-IR) spectroscopy; SEM analysis of NCColHA hydrogel with higher magnification; interfaces between the NCColHA hydrogel-coated area and the uncoated area; cytotoxicity of Col-N_3, HA-N_3, and NCs-DBCO; images of cell migration assay of Figure 3f after 24 h; CK14 expression in epithelial layers in *ex vivo* rabbit cornea; scheme for overall processes of *in vivo* efficacy study; whole rabbit eye images examined in *in vivo* study; OCT images of normal rabbit cornea; Tuj-1 expression in *in vivo* rabbit cornea on day 56; and collagen I expression in *in vivo* rabbit cornea on day 56 (PDF)

AUTHOR INFORMATION

Corresponding Author

David Myung − *Department of Ophthalmology, Spencer Center for Vision Research, Byers Eye Institute, Stanford University, Palo Alto, California 94304, United States; Department of Chemical Engineering, Stanford University, Stanford, California 94305, United States; VA Palo Alto HealthCare System, Palo Alto, California 94304, United States;* orcid.org/0000-0002-7980-3070; Email: djmyung@stanford.edu

Authors

Nae-Won Kang − *Department of Ophthalmology, Spencer Center for Vision Research, Byers Eye Institute, Stanford University, Palo Alto, California 94304, United States*

Kyeongwoo Jang − *Department of Ophthalmology, Spencer Center for Vision Research, Byers Eye Institute, Stanford University, Palo Alto, California 94304, United States;* orcid.org/0000-0002-3665-2698

Euisun Song − *Department of Ophthalmology, Spencer Center for Vision Research, Byers Eye Institute, Stanford University, Palo Alto, California 94304, United States*

Uiyoung Han − *Department of Ophthalmology, Spencer Center for Vision Research, Byers Eye Institute, Stanford University, Palo Alto, California 94304, United States*

Youngyoon Amy Seo − *Department of Ophthalmology, Spencer Center for Vision Research, Byers Eye Institute, Stanford University, Palo Alto, California 94304, United States*

Fang Chen − *Department of Ophthalmology, Spencer Center for Vision Research, Byers Eye Institute, Stanford University, Palo Alto, California 94304, United States*

Thitima Wungcharoen − *Department of Ophthalmology, Spencer Center for Vision Research, Byers Eye Institute, Stanford University, Palo Alto, California 94304, United States*

Sarah C. Heilshorn − *Department of Materials Science and Engineering, Stanford University, Stanford, California 94305, United States;* orcid.org/0000-0002-9801-6304

Complete contact information is available at: https://pubs.acs.org/10.1021/acsnano.4c02345

Author Contributions

The manuscript was written through contributions of all authors. All authors have given approval to the final version of the manuscript.

Notes

The authors declare the following competing financial interest(s): Authors N.K. and D.M. declare a patent application on the material technology described in this study.

ACKNOWLEDGMENTS

N.K. was supported by Basic Science Research Program through the National Research Foundation of Korea (NRF) funded by the Ministry of Education (RS-2023-00247051). This work was supported by a departmental core grant from Research to Prevent Blindness (RPB) as well as funding from the National Eye Institute (NIH R01 EY033363-03, R01 EY035697, and P30 EY026877) and the Harrington Discovery Institute Scholar-Innovator Award Program. Experiments were also performed in the Stanford Nano Shared Facilities and the Stanford School of Engineering Soft Materials Facility. Fang Chen was supported by the National Eye Institute (K99EY034168).

REFERENCES

(1) Sadtler, K.; Singh, A.; Wolf, M. T.; Wang, X.; Pardoll, D. M.; Elisseeff, J. H. Design, Clinical Translation and Immunological Response of Biomaterials in Regenerative Medicine. *Nat. Rev. Mater.* **2016**, *1*, 16040.

(2) Ueno, Y.; Nomura, R.; Hiraoka, T.; Kinoshita, K.; Ohara, M.; Oshika, T. Comparison of Corneal Irregular Astigmatism by The Type of Corneal Regular Astigmatism. *Sci. Rep.* **2021**, *11*, 15769.

(3) Thia, Z. Z.; Ho, Y. T.; Shih, K. C.; Tong, L. New Developments in The Management of Persistent Corneal Epithelial Defects. *Surv. Ophthalmol.* **2023**, *68*, 1093.

(4) Khosravimelal, S.; Mobaraki, M.; Eftekhari, S.; Ahearne, M.; Seifalian, A. M.; Gholipourmalekabadi, M. Hydrogels as Emerging Materials for Cornea Wound Healing. *Small* **2021**, *17*, 2006335.

(5) Cao, H.; Duan, L.; Zhang, Y.; Cao, J.; Zhang, K. Current Hydrogel Advances in Physicochemical and Biological Response-Driven Biomedical Application Diversity. *Signal Transduction Targeted Ther.* **2021**, *6*, 426.

(6) Palchesko, R. N.; Carrasquilla, S. D.; Feinberg, A. W. Natural Biomaterials for Corneal Tissue Engineering, Repair, and Regeneration. *Adv. Healthcare Mater.* **2018**, *7*, 1701434.

(7) Li, M.; Wei, R.; Liu, C.; Fang, H.; Yang, W.; Wang, Y.; Xian, Y.; Zhang, K.; He, Y.; Zhou, X. A "T.E.S.T." Hydrogel Bioadhesive Assisted by Corneal Cross-Linking for in situ Sutureless Corneal Rrepair. *Bioact. Mater.* **2023**, *25*, 333−346.

(8) Gouveia, R. M.; Lepert, G.; Gupta, S.; Mohan, R. R.; Paterson, C.; Connon, C. J. Assessment of Corneal Substrate Biomechanics and Its Effect on Epithelial Stem Cell Maintenance and Differentiation. *Nat. Commun.* **2019**, *10*, 1496.

(9) Shen, X.; Li, S.; Zhao, X.; Han, J.; Chen, J.; Rao, Z.; Zhang, K.; Quan, D.; Yuan, J.; Bai, Y. Dual-Crosslinked Regenerative Hydrogel for Sutureless Long-term Repair of Corneal Defect. *Bioact. Mater.* **2023**, *20*, 434−448.

(10) Li, L.; Lu, C.; Wang, L.; Chen, M.; White, J.; Hao, X.; McLean, K. M.; Chen, H.; Hughes, T. C. Gelatin-Based Photocurable Hydrogels for Corneal Wound Repair. *ACS Appl. Mater. Interfaces* **2018**, *10*, 13283−13292.

(11) Fernandes-Cunha, G. M.; Jeong, S. H.; Logan, C. M.; Le, P.; Mundy, D.; Chen, F.; Chen, K. M.; Kim, M.; Lee, G.-H.; Na, K.-S.; Hahn, S. K.; Myung, D. Supramolecular Host-Guest Hyaluronic Acid

Hydrogels Enhance Corneal Wound Healing Through Dynamic Spatiotemporal Effects. *Ocul Surf.* **2022**, *23*, 148−161.
(12) Rafat, M.; Li, F.; Fagerholm, P.; Lagali, N. S.; Watsky, M. A.; Munger, R.; Matsuura, T.; Griffith, M. PEG-stabilized Carbodiimide Crosslinked Collagen−Chitosan Hydrogels for Corneal Tissue Engineering. *Biomaterials* **2008**, *29*, 3960−3972.
(13) Goodarzi, H.; Jadidi, K.; Pourmotabed, S.; Sharifi, E.; Aghamollaei, H. Preparation and in vitro Characterization of Cross-Linked Collagen−Gelatin Hydrogel Using EDC/NHS for Corneal Tissue Engineering Applications. *Int. J. Biol. Macromol.* **2019**, *126*, 620−632.
(14) Sletten, E. M.; Bertozzi, C. R. Bioorthogonal Chemistry: Fishing for Selectivity in a Sea of Functionality. *Angew. Chem., Int. Ed. Engl.* **2009**, *48*, 6974−6998.
(15) Madl, C. M.; Heilshorn, S. C. Bioorthogonal Strategies for Engineering Extracellular Matrices. *Adv. Funct. Mater.* **2018**, *28*, 1706046.
(16) Li, Y.; Wang, X.; Han, Y.; Sun, H.-Y.; Hilborn, J.; Shi, L. Click Chemistry-Based Biopolymeric Hydrogels for Regenerative Medicine. *Biomed. Mater.* **2021**, *16*, No. 022003.
(17) Madl, C. M.; Katz, L. M.; Heilshorn, S. C. Bio-Orthogonally Crosslinked, Engineered Protein Hydrogels with Tunable Mechanics and Biochemistry for Cell Encapsulation. *Adv. Funct. Mater.* **2016**, *26*, 3612.
(18) Jiang, Y.; Chen, J.; Deng, C.; Suuronen, E. J.; Zhong, Z. Click Hydrogels, Microgels and Nanogels: Emerging Platforms for Drug Delivery and Tissue Engineering. *Biomaterials* **2014**, *35*, 4969−4985.
(19) Chen, F.; Le, P.; Fernandes-Cunha, G. M.; Heilshorn, S. C.; Myung, D. Bio-Orthogonally Crosslinked Hyaluronate-Collagen Hydrogel for Suture-Free Corneal Defect Repair. *Biomaterials* **2020**, *255*, No. 120176.
(20) Lee, H. J.; Fernandes-Cunha, G. M.; Na, K.; Hull, S. M.; Myung, D. Bio-Orthogonally Crosslinked, in situ Forming Corneal Stromal Tissue Substitute. *Adv. Healthcare Mater.* **2018**, *7*, 1800560.
(21) Zhang, H.; Zhu, Y.; Qu, L.; Wu, H.; Kong, H.; Yang, Z.; Chen, D.; Makila, E.; Salonen, J.; Santos, H. A.; Hai, M.; Weitz, D. A. Gold Nanorods Conjugated Porous Silicon Nanoparticles Encapsulated in Calcium Alginate Nano Hydrogels Using Microemulsion Templates. *Nano Lett.* **2018**, *18*, 1448−1453.
(22) Pérez-Rafael, S.; Ivanova, K.; Stefanov, I.; Puiggalí, J.; del Valle, L. J.; Todorova, K.; Dimitrov, P.; Hinojosa-Caballero, D.; Tzanov, T. Nanoparticle-Driven Self-Assembling Injectable Hydrogels Provide a Multi-Factorial Approach for Chronic Wound Treatment. *Acta Biomater.* **2021**, *134*, 131−143.
(23) Grosskopf, A. K.; Roth, G. A.; Smith, A. A. A.; Gale, E. C.; Hernandez, H. L.; Appel, E. A. Injectable Supramolecular Polymer−Nanoparticle Hydrogels Enhance Human Mesenchymal Stem Cell Delivery. *Bioeng. Transl. Med.* **2020**, *5*, e10147.
(24) Grosskopf, A. K.; Saouaf, O. A.; Lopez Hernandez, H.; Appel, E. A. Gelation and Yielding Behavior of Polymer−Nanoparticle Hydrogels. *J. Polym. Sci.* **2021**, *59*, 2854−2866.
(25) Appel, E. A.; Tibbitt, M. W.; Webber, M. J.; Mattix, B. A.; Veiseh, O.; Langer, R. Self-assembled hydrogels utilizing polymer−nanoparticle interactions. *Nat. Commun.* **2015**, *6*, 6295.
(26) Wang, Q.; Zhang, Y.; Ma, Y.; Wang, M.; Pan, G. Nano-Crosslinked Dynamic Hydrogels for Biomedical Application. *Mater. Today Bio.* **2023**, *20*, No. 100640.
(27) Jiang, Y.; Krishnan, N.; Heo, J.; Fang, R. H.; Zhang, L. Nanoparticle−Hydrogel Superstructures for Biomedical Applications. *J. Controlled Release* **2020**, *324*, 505−521.
(28) Kang, N.-W.; Lee, J.-Y.; Kim, D.-D. Hydroxyapatite-Binding Albumin Nanoclusters for Enhancing Bone Tumor Chemotherapy. *J. Controlled Release* **2022**, *342*, 111−121.
(29) Yoo, S.-Y.; Mun, Y.-H.; Kang, N.-W.; Koo, J. M.; Lee, D. H.; Yoo, J. H.; Lee, S. M.; Koh, S.; Park, J. C.; Kim, T.; Shin, E. K.; Lee, H. S.; Sim, J.; Kang, K. W.; Kim, S. K.; Cho, C.-W.; Kim, M. G.; Kim, D.-D.; Lee, J.-Y. Enhancement of the Therapeutic Efficacy of the MAP Regimen Using Thiamine Pyrophosphate-Decorated Albumin Nanoclusters in Osteosarcoma Treatment. *Bioeng. Transl. Med.* **2023**, *8*, e10472.
(30) Porcello, A.; Gonzalez-Fernandez, P.; Jordan, O.; Allemann, E. Nanoforming Hyaluronan-Based Thermoresponsive Hydrogels: Optimized and Tunable Functionality in Osteoarthritis Management. *Pharmaceutics* **2022**, *14*, 659.
(31) Han, S.-S.; Yoon, H. Y.; Yhee, J. Y.; Cho, M. O.; Shim, H.-E.; Jeong, J.-E.; Lee, D.-E.; Kim, K.; Guim, H.; Lee, J. H.; Huh, K. M.; Kang, S.-W. In Situ Cross-Linkable Hyaluronic Acid Hydrogels Using Copper Free Click Chemistry for Cartilage Tissue Engineering. *Polym. Chem.* **2018**, *9*, 20.
(32) Pushpamalar, V.; Langford, S. J.; Ahmad, M.; Hashim, K.; Lim, Y. Y. Preparation of Carboxymethyl Sago Pulp Hydrogel from Sago Waste by Electron Beam Irradiation and Swelling Behavior in Water and Various pH Media. *J. Appl. Polym. Sci.* **2013**, *128*, 451.
(33) Yazdanpanah, G.; Shen, X.; Nguyen, T.; Anwar, K. N.; Jeon, O.; Jiang, Y.; Pachenari, M.; Pan, Y.; Shokuhfar, T.; Rosenblatt, M. I.; Alsberg, E.; Djalilian, A. R. A Light-Curable and Tunable Extracellular Matrix Hydrogel for in situ Suture-Free Corneal Repair. *Adv. Funct. Mater.* **2022**, *32*, 2113383.
(34) Wang, F.; Zhang, W.; Qiao, Y.; Shi, D.; Hu, L.; Cheng, J.; Wu, J.; Zhao, L.; Li, D.; Shi, W.; Xie, L.; Zhou, Q. ECM-Like Adhesive Hydrogel for the Regeneration of Large Corneal Stromal Defects. *Adv. Healthcare Mater.* **2023**, *12*, 2300192.
(35) Ramli, H.; Zainal, N. F. A.; Hess, M.; Chan, C. H. Basic Principle and Good Practices of Rheology for Polymers for Teachers and Beginners. *Chem. Teach. Int.* **2022**, *4*, 307−326.
(36) Yin, Q.; Luo, W.; Mallajosyula, V.; Bo, Y.; Guo, J.; Xie, J.; Sun, M.; Verma, R.; Li, C.; Constantz, C. M.; Wagar, L. E.; Li, J.; Sola, E.; Gupta, N.; Wang, C.; Kask, O.; Chen, X.; Yuan, X.; Wu, N. C.; Rao, J.; Chien, Y.-h.; Cheng, J.; Pulendran, B.; Davis, M. M. A TLR7-Nanoparticle Adjuvant Promotes a Broad Immune Response Against Heterologous Strains of Influenza and SARS-CoV-2. *Nat. Mater.* **2023**, *22*, 380−390.
(37) Li, J.; Mooney, D. J. Designing Hydrogels for controlled Drug Delivery. *Nat. Rev. Mater.* **2016**, *1*, 16071.
(38) Qian, Y.; Xu, K.; Shen, L.; Dai, M.; Zhao, Z.; Zheng, Y.; Wang, H.; Xie, H.; Wu, X.; Xiao, D.; Zheng, Q.; Zhang, J.; Song, Y.; Shen, J.; Chen, W. Dopamine-Based High-Transparent Hydrogel as Bioadhesive for Sutureless Ocular Tissue Repair. *Adv. Funct. Mater.* **2023**, *33*, 2300707.
(39) Zhan, Y.; Fu, W.; Xing, Y.; Ma, X.; Chen, C. Advances in Versatile Anti-Swelling Polymer Hydrogels. *Mater. Sci. Eng., C* **2021**, *127*, No. 112208.
(40) Singh, V.; Tiwari, A.; Kethiri, A. R.; Sangwan, V. S. Current Perspectives of Limbal-Derived Stem Cells and Its Application in Ocular Surface Regeneration and Limbal Stem Cell Transplantation. *Stem Cells Transl. Med.* **2021**, *10*, 1121−1128.
(41) Spix, J. K.; Chay, E. Y.; Block, E. R.; Klarlund, J. K. Hepatocyte Growth Factor Induces Epithelial Cell Motility Through Transactivation of the Epidermal Growth Factor Receptor. *Exp. Cell Res.* **2007**, *313*, 3319−3325.
(42) Sun, Y.; Chan, J.; Bose, K.; Tam, C. Simultaneous Control of Infection and Inflammation with Keratin-Derived Antibacterial Peptides Targeting TLRs and Co-Receptors. *Sci. Transl. Med.* **2023**, *15*, eade2909.
(43) Fernandes-Cunha, G. M.; Brunel, L. G.; Arboleda, A.; Manche, A.; Seo, Y. A.; Logan, C.; Chen, F.; Heilshorn, S. C.; Myung, D. Collagen Gels Crosslinked by Photoactivation of Riboflavin for the Repair and Regeneration of Corneal Defects. *ACS Appl. Bio Mater.* **2023**, *6*, 1787−1797.
(44) Yu, F. X.; Guo, J.; Zhang, Q. Expression and Distribution of Adhesion Molecule CD44 in Healing Corneal Epithelia. *Invest. Ophthalmol. Visual Sci.* **1998**, *39*, 710−717.
(45) Figueira, E. C.; Di Girolamo, N.; Coroneo, M. T.; Wakefield, D. The Phenotype of Limbal Epithelial Stem Cells. *Invest. Ophthalmol. Visual Sci.* **2007**, *48*, 144−156.

https://doi.org/10.1021/acsnano.4c02345
ACS Nano 2024, 18, 21925−21938

(46) Kammergruber, E.; Rahn, C.; Nell, B.; Gabner, S.; Egerbacher, M. Morphological and Immunohistochemical Characteristics of the Equine Corneal Epithelium. *Vet. Ophthalmol.* **2019**, *22*, 778.
(47) Chen, B.; Mi, S.; Wright, B.; Connon, C. J.; Chakravarti, S. Investigation of K14/K5 as a Stem Cell Marker in the Limbal Region of the Bovine Cornea. *PLoS One* **2010**, *5*, e13192.
(48) Park, M.; Richardson, A.; Pandzic, E.; Lobo, E. P.; Whan, R.; Watson, S. L.; Lyons, J. G.; Wakefield, D.; Di Girolamo, N. Visualizing the Contribution of Keratin-14+ Limbal Epithelial Precursors in Corneal Wound Healing. *Stem Cell Rep.* **2018**, *12*, 14.
(49) Yi, X.-J.; Wang, Y.; Yu, F.-S. X. Corneal Epithelial Tight Junctions and Their Response to Lipopolysaccharide Challenge. *Invest. Ophthalmol. Visual Sci.* **2000**, *41*, 4093−4100.
(50) Reza, H. M.; Ng, B.-Y.; Gimeno, F. L.; Phan, T. T.; Ang, L. P.-K. Umbilical Cord Lining Stem Cells as a Novel and Promising Source for Ocular Surface Regeneration. *Stem Cell Rev. And Rep.* **2011**, *7*, 935.
(51) Rana, D.; Desai, N.; Salave, S.; Karunakaran, B.; Giri, J.; Benival, D.; Gorantla, S.; Kommineni, N. Collagen-Based Hydrogels for the Eye: A Comprehensive Review. *Gels* **2023**, *9*, 643.
(52) Li, S.; Ma, X.; Zhang, Y.; Qu, Y.; Wang, L.; Ye, L. Applications of Hydrogel Materials in Different Types of Corneal Wounds. *Surv. Ophthalmol.* **2023**, *68*, 746.
(53) Gong, Q.; Zhao, Y.; Qian, T.; Wang, H.; Li, Z. Functionalized hydrogels in ophthalmic applications: Ocular inflammation, corneal injuries, vitreous substitutes and intravitreal injection. *Mater. Des.* **2022**, *224*, No. 111277.
(54) de Rojas Silva, M. V.; Álvarez de Toledo, J.; Tobío Ruibal, A. Mechanical Removal of Epithelial Hyperplasia Leads to Successful Treatment of Irregular Astigmatism. *BMC Ophthalmol.* **2023**, *23*, 122.
(55) Wilson, S. E.; Mohan, R. R.; Hong, J.-W.; Lee, J.-S.; Choi, R.; Mohan, R. R. Mechanical Removal of Epithelial Hyperplasia Leads to Successful Treatment of Irregular Astigmatism. *Arch. Ophthalmol.* **2001**, *119*, 889−896.
(56) Kivanany, P. B.; Grose, K. C.; Tippani, M.; Su, S.; Petroll, W. M. Assessment of Corneal Stromal Remodeling and Regeneration After Photorefractive Keratectomy. *Sci. Rep.* **2018**, *8*, 12580.
(57) Chen, J.; Li, Z.; Zhang, L.; Ou, S.; Wang, Y.; He, X.; Zou, D.; Jia, C.; Hu, Q.; Yang, S.; Li, X.; Li, J.; Wang, J.; Sun, H.; Chen, Y.; Zhu, Y.-T.; Tseng, S. C. G.; Liu, Z.; Li, W. Descemet's Membrane Supports Corneal Endothelial Cell Regeneration in Rabbits. *Sci. Rep.* **2017**, *7*, 6983.
(58) Gauthier, C. A.; Holden, B. A.; Epstein, D.; Tengroth, B.; Fagerholm, P.; Hamberg-Nystrom, H. Role of Epithelial Hyperplasia in Regression Following Photorefractive Keratectomy. *Br. J. Ophthalmol.* **1996**, *80*, 545.
(59) Jeon, K.-I.; Hindman, H. B.; Bubel, T.; McDaniel, T.; DeMagistris, M.; Callan, C.; Huxlin, K. R. Corneal Myofibroblasts Inhibit Regenerating Nerves During Wound Healing. *Sci. Rep.* **2018**, *8*, 12945.
(60) Lee, S.; Choi, K.; Ahn, H.; Song, K.; Choe, J.; Lee, I. TuJ1 (Class III b-tubulin) Expression Suggests Dynamic Redistribution of Follicular Dendritic Cells in Lymphoid Tissue. *Eur. J. Cell Biol.* **2005**, *84*, 453.

https://doi.org/10.1021/acsnano.4c02345
ACS Nano 2024, 18, 21925−21938